

# Domain-Specific Chaperone-Induced Expansion Is Required for $\beta$ -Actin Folding: A Comparison of $\beta$ -Actin Conformations upon Interactions with GroEL and Tail-less Complex Polypeptide 1 Ring Complex (TRiC)<sup>†</sup>

Laila Villebeck,<sup>‡</sup> Satish Babu Moparthi,<sup>§</sup> Mikael Lindgren,<sup>||</sup> Per Hammarström,<sup>§</sup> and Bengt-Harald Jonsson<sup>\*,‡</sup>

*Divisions of Molecular Biotechnology and of Chemistry, IFM, Linköping University, 581 83 Linköping, Sweden, and Department of Physics, The Norwegian University of Science and Technology, 7491 Trondheim, Norway*

*Received April 6, 2007; Revised Manuscript Received August 29, 2007*

**ABSTRACT:** Actin, an abundant cytosolic protein in eukaryotic cells, is dependent on the interaction with the chaperonin tail-less complex polypeptide 1 ring complex (TRiC) to fold to the native state. The prokaryotic chaperonin GroEL also binds non-native  $\beta$ -actin, but is unable to guide  $\beta$ -actin toward the native state. In this study we identify conformational rearrangements in  $\beta$ -actin, by observing similarities and differences in the action of the two chaperonins. A cooperative collapse of  $\beta$ -actin from the denatured state to an aggregation-prone intermediate is observed, and insoluble aggregates are formed in the absence of chaperonin. In the presence of GroEL, however, >90% of the aggregation-prone actin intermediate is kept in solution, which shows that the binding of non-native actin to GroEL is effective. The action of GroEL on bound fluorescein-labeled  $\beta$ -actin was characterized, and the structural rearrangement was compared to the case of the  $\beta$ -actin–TRiC complex, employing the homo fluorescence resonance energy transfer methodology previously used [Villebeck, L., Persson, M., Luan, S.-L., Hammarström, P., Lindgren, M., and Jonsson, B.-H. (2007) *Biochemistry* 46 (17), 5083–93]. The results suggest that the actin structure is rearranged by a “binding-induced expansion” mechanism in both TRiC and GroEL, but that binding to TRiC, in addition, causes a large and specific separation of two subdomains in the  $\beta$ -actin molecule, leading to a distinct expansion of its ATP-binding cleft. Moreover, the binding of ATP and GroES has less effect on the GroEL-bound  $\beta$ -actin molecule than the ATP binding to TRiC, where it leads to a major compaction of the  $\beta$ -actin molecule. It can be concluded that the specific and directed rearrangement of the  $\beta$ -actin structure, seen in the natural  $\beta$ -actin–TRiC system, is vital for guiding  $\beta$ -actin to the native state.

The chaperonins belong to a family of large, multimeric, barrel-shaped chaperones that assist in the folding, or prevent misfolding, of non-native proteins in vivo. Chaperonins are present in all three kingdoms of life, and the most studied chaperonins are GroEL from eubacteria, the thermosome from archaea, and the tail-less complex polypeptide 1 (TCP-1)<sup>1</sup> ring complex (TRiC) from eukaryotic cells (reviewed in refs 1–6). The chaperonin family is divided into two classes: The group I chaperonins, found in eubacteria and organelles with prokaryotic origin, and group II chaperonins, present in archaea and in the cytoplasm of eukaryotes. The group I and group II chaperonins have the general architec-

ture and their role of assisting in the folding of target proteins in common, but there are also many differences between the chaperonin groups. The group I chaperonins are homooligomeric complexes composed of two identical rings stacked back to back and work in conjunction with a single-ring co-chaperonin. The group II chaperonins form two identical rings that are heterooligomeric and composed of eight- or nine-membered rings. Moreover, group II chaperonins are independent of a co-chaperonin.

The mechanism by which the chaperonins work and how the target protein is affected by the conformational changes that occur in the chaperonin during the folding cycle are still under intense investigation. In our previous work, spectroscopic and thermodynamic studies on the bacterial chaperonin GroEL indicated that the chaperonin works by a binding-induced expansion mechanism. The methods of EPR (electron spin resonance) spectroscopy (7) and fluorescence resonance energy transfer (FRET) measurements (8) showed that binding to GroEL forces a bound target protein to expand its hydrophobic core. It was also shown that the mere binding of the target protein to GroEL induced conformational changes in the chaperonin, consequently leading to rearrangements of the target protein (9). This binding-induced expansion, completely independent of ATP and GroES, was

<sup>†</sup> We are grateful for financial support from the NanoMat program of the Norwegian Science Research Council to M.L. and from the Swedish Research Council to B.-H.J. and P.H. A Marie Curie Early Stage Research Training Fellowship under contract number MEST-CT-2004-504272 to S.B.M. is also gratefully acknowledged.

<sup>\*</sup> To whom correspondence should be addressed. Phone: +46 13 288935 or +46 703974520. Fax: +46 13 122587. E-mail: nalle@ifm.liu.se.

<sup>‡</sup> Division of Molecular Biotechnology, IFM, Linköping University.

<sup>§</sup> Division of Chemistry, IFM, Linköping University.

<sup>||</sup> The Norwegian University of Science and Technology.

<sup>1</sup> Abbreviations: TRiC, TCP-1 ring complex; TCP-1, tail-less complex polypeptide 1; FRET, fluorescence resonance energy transfer; EPR, electron spin resonance; GuHCl, guanidinium chloride; AMP-PNP, adenylyl imidodiphosphate; 6-IAF, 6-iodoacetamidofluorescein; DTT, dithiothreitol.

concluded to give the target protein a chance to correct a misfolded substructure into the correct one, which in turn leads to an increased yield of native protein (10, 11). Further support comes from a recent study by Lin (12). Using FRET measurements, it was shown that, when the target protein ribulose-1,5-bisphosphate carboxylase/oxygenase (Rubisco) binds to GroEL in the absence of ATP, Rubisco is stretched by an unfolding mechanism. Binding of ATP and the co-chaperonin GroES leads to a compaction of the bound substrate. These results support the hypothesis that the chaperonins work by a "binding-induced expansion" mechanism, in contrast to the "Anfinsen cage" model, where the chaperonin is just a passive container where the target protein is protected from the crowded environment in the cell during the folding. The binding-induced expansion is also different from the suggested "forced unfolding" mechanism, where it is proposed that the binding of ATP and GroES to GroEL contributes to the energy needed for an active stretching/unfolding of the bound target protein.

The eukaryotic chaperonin TRiC has been suggested to be more specific in recognizing and binding of target proteins than its bacterial counterpart. Two proteins (actins and tubulins) were early proposed to be the main substrates of TRiC (13, 14). Since then, the list of proteins interacting with TRiC has grown larger (15), but still most studies on the chaperonin TRiC involve actin and/or tubulin as target proteins. We have recently presented a study of the actin-TRiC interaction, where we used homo-FRET to measure distances, which showed that  $\beta$ -actin is actively stretched by binding-induced expansion (16). It was concluded that the chaperonin unfolding mechanism is evolutionarily conserved among the chaperonins.

$\beta$ -Actin is unable to fold to its native structure without assistance from the chaperonin TRiC (13, 14). It has, however, earlier also been shown that a non-native actin intermediate is recognized by and bound to GroEL. However, this is not a natural system, and the prokaryotic chaperonin is not able to guide actin to its native state (17). It has been proposed that the two different chaperonins recognize different folding intermediates of the target protein (18).

In this study, we use a pseudo-wild-type variant of  $\beta$ -actin (previously described by us in ref 16) in which the natural cysteine residues have been substituted by alanine to allow the introduction of specific cysteine residues as handles for the fluorescent probe fluorescein. From observing similarities and differences in the action of the two chaperonins, conformational rearrangements in  $\beta$ -actin, which are specific for TRiC, are identified. A distance map of actin bound to the GroEL chaperonin is obtained and is compared to new data in addition to previously obtained results on actin bound to TRiC. The results from the homo-FRET measurements suggest that the actin structure is rearranged by a binding-induced expansion mechanism in both TRiC and GroEL, but that binding to TRiC, in addition, causes a large separation of two subdomains, leading to an expansion of the ATP-binding cleft in  $\beta$ -actin. Also, the pronounced compaction of TRiC-bound actin, after addition of AMP-PNP to the chaperonin complex, is different and more dramatic than when AMP-PNP and GroES are added to the actin-GroEL complex.

## EXPERIMENTAL PROCEDURES

**Production and Purification of Proteins.** Engineered actin variants were produced and purified as described by Villebeck et al. (16). GroEL was purified according to Persson et al. (19), and its chaperone activity was ascertained by monitoring the effects on the refolding of human carbonic anhydrase II. TRiC was purified as described by Villebeck (16).

**Fluorescein Labeling of Engineered Actin Variants.** The labeling of the actin variants with fluorescein was performed as described by Villebeck et al. (16). The degree of labeling was calculated by determination of free thiol groups at 412 nm, using Ellman's reagent and  $\epsilon_{412} = 14\,150\text{ M}^{-1}\text{ cm}^{-1}$  (20) and was determined to be >90% for all variants.

**Fluorescein Steady-State Fluorescence Anisotropy and Homo-FRET Measurements.** Fluorescence measurements were performed on 400  $\mu\text{L}$  samples with a final actin concentration of 0.4 and 1.6  $\mu\text{M}$  GroEL in 0.1 M Tris-HCl, 10 mM KCl, 10 mM  $\text{MgCl}_2$ , pH 7.5. The samples were prepared as follows: After addition of DTT to GroEL to a final concentration of 1 mM, the sample was incubated at 30 °C for 15 min. Labeled and denatured actin was mixed with unlabeled, denatured actin in a 1:4 molar ratio and was subsequently diluted 125–300-fold into the GroEL-containing solution, adding 1  $\mu\text{L}$  at a time. The final GuHCl concentration was 12–32 mM in all of the GroEL-containing samples. The binding reaction was allowed to proceed for 45 min at 30 °C. Insoluble aggregates were removed by centrifugation at 17700g for 5 min. The steady-state fluorescence anisotropy spectra were recorded on a Hitachi F-4500 spectrofluorometer at 21 °C, with slits of 5 and 10 nm for emission and excitation, respectively. The emission wavelength was set to 524 nm, and the excitation spectra were collected in the region 460–510 nm at four different polarization configurations, VV, VH, HH, and HV. After the measurements on the actin-GroEL complex, AMP-PNP was added to a final concentration of 160  $\mu\text{M}$ , and the sample was incubated at 30 °C for 15 min before recording of the spectra. Thereafter, GroES was added to a final concentration of 2  $\mu\text{M}$ , the sample was incubated at 30 °C for 15 min, and the last spectra were recorded. Similar measurements were also conducted on selected actin variants diluted into 4, 1, 0.5, 0.3, 0.2, and 0.017 M GuHCl, all containing 0.1 M Tris-HCl, 10 mM KCl, 10 mM  $\text{MgCl}_2$ , pH 7.5, and 0.4  $\mu\text{M}$  actin. The distances between labeled positions were determined from the measurements of homo-FRET as described earlier (16).

## RESULTS AND DISCUSSION

Site-directed mutagenesis has been used to make site-specific labeling of chosen positions throughout the  $\beta$ -actin molecule possible (Figure 1A). The positions were chosen to report on distances between subdomains 2 and 4 (positions 39–246), within subdomain 4 (positions 246–261), between subdomains 1 and 4 (positions 137–261 and 86–261), and between subdomains 1 and 3 (positions 288–354). In total, seven single variants (R39C, W86C, Q137C, Q246C, L261C, D288C, and Q354C) and five double variants (R39C/Q246C, W86C/L261C, Q137C/L261C, Q246C/L261C, and D288C/Q354C) were constructed, expressed, purified, and labeled with the fluorophore 6-iodoacetamidofluorescein (6-IAF),

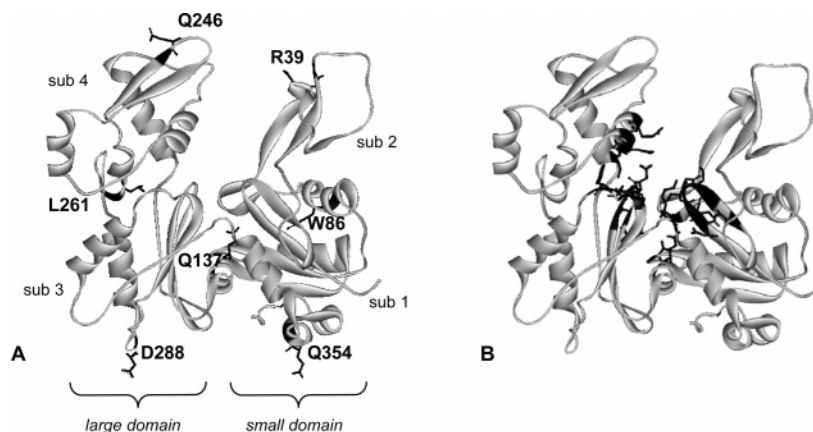


FIGURE 1: Structure of native  $\beta$ -actin. (A) The positions chosen for site-specific labeling are marked with black stick representations. (B) The amino acids involved in the nucleotide-binding site are highlighted in black (41). The ribbon representations are based on the crystal structure of bovine  $\beta$ -actin (PDB accession number 1HLU).

hereafter referred to as fluorescein. The homo-FRET methodology previously used to study the actin–TRiC complexes (16) was employed in this study to determine distances between labeled positions in  $\beta$ -actin: (a) under denaturing conditions, (b) in an aggregated state, and (c) in the actin–TRiC/ADP, actin–TRiC/AMP-PNP, actin–GroEL, and actin–GroEL/ES/AMP-PNP complexes. Fluorescein has a very small Stokes shift, which leads to easily obtainable homo-FRET between fluorescein molecules that are 20–70 Å apart (21). The homo-FRET is observed as an apparent lower anisotropy at shorter wavelengths and can be used to calculate the distance between two fluorescein molecules, as described in refs 16 and 21. The obtained distances were used to report on rearrangements in the  $\beta$ -actin molecule under different conditions as described in the following sections. A comparative analysis allows identification of similarities and differences in the action of two chaperonins.

*In the Absence of Chaperonin Non-Native Actin Intermediates Form Aggregates.* Fluorescein is a fluorophore that is sensitive to rotation and can be used to report on motion by anisotropy measurements (16, 21). Fluorescence anisotropy is dependent both on the size of the molecule (or complex) where the probe (fluorescein) is attached (smaller size yields faster tumbling and thus lower anisotropy) and on the mobility of the probe itself (fast rotation yields low anisotropy). Denatured actin displays a low anisotropy, 0.08–0.10 in 4 M GuHCl (shown for L261C in Figure 2F), indicating fast tumbling of a monomeric actin molecule and relatively free rotation of the fluorescein probe. When GuHCl-denatured actin is subjected to folding conditions, through dilution with buffer, it is unable to reach its native state. It forms folding intermediates that are prone to aggregation. These aggregates can be seen by the eye as a marked scattering of light. The observed higher anisotropy values (typically 0.15–0.16) (shown for L261C in Figure 2F), as compared to the corresponding values for denatured actin, also show the presence of aggregates. The low stability of the labeled actin molecules in combination with the strong tendency to form aggregates upon refolding hinders production and purification of monomeric actin molecules with native or close to native structure for the labeled actin variants (16, 42). Thus, the question of whether TRiC or GroEL interacts with actin having native or close to native structure cannot be resolved with the approach taken in this study.

*Distance Determinations on “Free” Actin Molecules.* In the actin aggregates mentioned above, there is a risk of homo-FRET between fluorescein probes, which are located in different actin molecules, “inter-actin homo-FRET”. This would interfere with the determination of the anisotropies and of the distances between labeled positions within the individual actin molecule. To make proper distance determinations on actin samples at GuHCl concentrations below 4 M, the risk of inter-actin homo-FRET has been minimized by mixing the labeled actin with a 4-fold excess of unlabeled actin before diluting the denatured protein into buffers of various GuHCl concentrations. This process leads to a high probability that labeled actin molecules have unlabeled actin as nearest neighbors and, as a consequence, that the homo-FRET measurements report on distances within the actin molecule itself and not between different actin molecules in an aggregate. This procedure was used in the GuHCl titration of actin variants R39C, Q246C, and R39C/Q246C (Figure 3A, described below), in the measurements of anisotropy on all variants at 0 M GuHCl (shown for variant L261C in Figure 2F), and in the homo-FRET-determined distances at 0 M GuHCl (Table 1 and Figure 4).

*Cooperative Collapse of the Actin Molecule as the Denaturant Is Removed.* As shown in previous (16) and present measurements, the actin molecule collapses into a more compact structure as it is diluted from 4 M GuHCl to 0 M GuHCl (Table 1). Here, a GuHCl titration on the R39C/Q246C variant and the appurtenant single variants was performed, and homo-FRET was measured on samples with the actin variants dissolved in 0.017–7.5 M GuHCl. The calculated distances were plotted against the concentration of GuHCl, and the result is presented in Figure 3A. The results show that the collapse from denatured actin to a non-native actin intermediate is cooperative. One may note that the cooperative compaction of the actin molecule is monitored by measuring distances, while the more common methods use various probes that sense changes in the chemical environment. At 0.3 M and lower, the actin molecule seems to have reached an intermediate state with a distance of about 45 Å between positions 39 and 246. The formation of aggregates is shown by the increase in anisotropy for all actin variants as the denaturant is removed (shown for variant L261C in Figure 2F).

*Does Aggregation Interfere with the Characterization of the Actin–Chaperonin Complexes?* In the absence of chap-



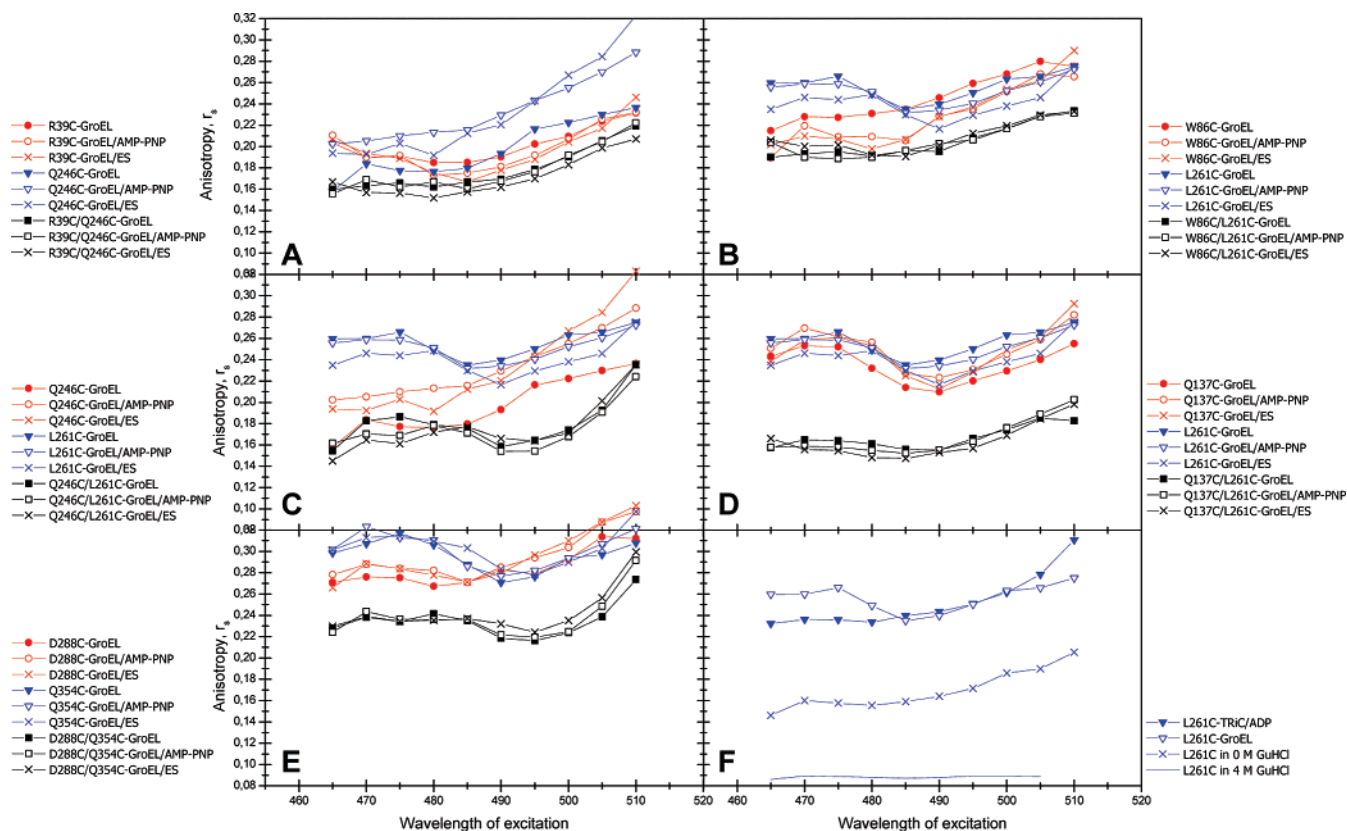


FIGURE 2: Steady-state anisotropy spectra for actin variants labeled with fluorescein. (A–E) Steady-state anisotropy spectra for the fluorescein-labeled actin double variants R39C/Q246C (A), W86C/L261C (B), Q246C/L261C (C), Q137C/L261C (D), and D288C/Q354C (E) with their respective single variants bound to GroEL (solid symbols), GroEL/AMP-PNP (open symbols), and GroEL/ES/AMP-PNP (multiplication signs). Where homo-FRET is present, the double variants have lower anisotropies than their corresponding single variants. (F) Representative steady-state anisotropy spectra for actin denatured in 4 M GuHCl (solid line), diluted from 4 M GuHCl into folding buffer (multiplication signs), bound to GroEL (open triangles), and bound to TRiC/ADP (solid triangles), illustrating how the anisotropy of fluorescein-labeled molecules or complexes is dependent on the size of the complex. The larger the complex, the higher the anisotropy.

eronins and under conditions that allow formation of the native state, the majority of the denatured actin molecules aggregate. To investigate whether the aggregation would obscure the determination of distances, in actin–chaperonin complexes, control experiments were performed. GuHCl-denatured actin was diluted by buffer to 0 M GuHCl. After centrifugation of these chaperonin-devoid actin samples, more than 90% of the fluorescence signal was lost compared to the samples where actin was kept in solution by binding to GroEL. To investigate whether monomeric and soluble actin molecules are released from the GroEL–actin complex or from the GroEL/ES/AMP-PNP–actin complex, the changes in signal intensity and steady-state anisotropy with time after formation of the complexes were investigated. The signal intensity and the anisotropy did not change over a time span of 3 h. Repeated centrifugation after 3 h altered neither the signal intensity nor the anisotropy, indicating that no aggregation-prone actin molecules are released from the chaperone complexes. These results are supported by the observation by Tian et al. (17) that actin–chaperone complexes are stable in the absence of ATP. Importantly, the loss of an emission signal after removal of actin aggregates by centrifugation ensures that, when the chaperonin-containing samples are being prepared, the aggregates are removed by centrifugation and the recorded homo-FRET emanates solely from chaperonin-bound actin. Thus, the actin molecules are rescued from aggregation in the experiments by the presence of TRiC or GroEL in the samples. Since neither

TRiC nor GroEL was removed by centrifugation at speeds which efficiently remove the aggregates, their size must be much larger than that of the chaperonins.

**Anisotropy Measurements Verify Binding of Actin to GroEL.** It is well-established that GroEL is promiscuous in its recognition of, and interaction with, target proteins. The interactions occur through conserved hydrophobic residues in the apical domains of the chaperonin (22, 23). The binding region presents plasticity and adjusts depending on which target protein is bound (24). TRiC, on the other hand, interacts with fewer proteins and has a specific recognition mechanism toward the target proteins. The eight different subunits are proposed to recognize and bind to different target proteins. Some groups report that the TRiC subunits interact with target proteins through polar and electrostatic interactions (25–28), while other groups report on interactions through hydrophobic interactions (29–31). However, the mechanism by which these distantly related chaperonins work, seems to be evolutionarily conserved by means of using binding-induced expansion to mechanically expand or rearrange a target molecule (7–9, 12, 16, 32) in such a way that a misfolded structure could be unraveled (10, 11), allowing subsequent refolding into the native structure. Also, the compaction mechanism of the target proteins in the subsequent ATP-binding step in the TRiC chaperonin cycle (16, 32) and the ATP + GroES-binding step in the GroEL chaperonin cycle (12) obviously is conserved through evolution. However, it is proposed that evolution has an effect on

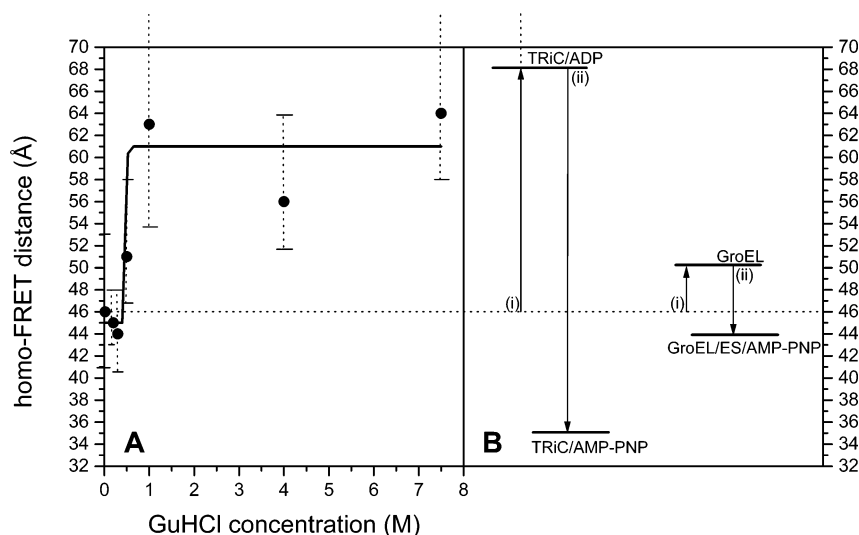


FIGURE 3: (A) GuHCl titration of R39C/Q246C where the distances at different GuHCl concentrations, 7.5, 4, 1, 0.5, 0.2, 0.1, and 0.017 M, are indicated. The titration shows a curve with a steep slope, which shows that the collapse of the unfolded actin molecule from 7.5 M GuHCl to the non-native, aggregation-prone actin intermediate is cooperative. (B) Schematic diagram illustrating the major distance changes (between positions 39 and 246) upon the interaction between actin and the chaperonins TRiC and GroEL. Arrows indicate (i) the increase in distance as the non-native actin intermediate binds to the chaperonin and (ii) the decrease in distance between positions 39 and 246 during the chaperonin folding cycle to TRiC/AMP-PNP or GroEL/ES/AMP-PNP. Vertical dashed lines in (A) represent the distance range appearing when the  $r_s$  values of the individual actin single variants are used as  $r_{01}$  (to calculate distance by homo-FRET) separately, one at a time. The dashed horizontal line represents the 39–246 distance (46 Å) in the actin intermediate at 0 M GuHCl, which is proposed to bind to TRiC/ADP or GroEL.

Table 1: Calculated Distances in  $\beta$ -Actin Variants in Different Environments

	steady-state FRET distance (Å)						
	4 M GuHCl	0 M GuHCl	TRiC/ADP	GroEL	TRiC/AMP-PNP	GroEL/AMP-PNP	GroEL/ES/AMP-PNP
R39C/Q246C (37) <sup>b</sup> (subs 2–4) <sup>c</sup>	>55 <sup>d</sup> (52–64) <sup>a,d</sup>	46 <sup>d</sup> (41–53) <sup>a,d</sup>	>68 <sup>d</sup> (57–) <sup>a,d</sup>	50 (48–51) <sup>a</sup>	35 <sup>d</sup> (33–38) <sup>a,d</sup>	45 (41–51) <sup>a</sup>	44 (41–48) <sup>a</sup>
W86C/L261C (33) <sup>b</sup> (subs 1–4) <sup>c</sup>	>55 <sup>d</sup> (64–) <sup>a,d</sup>	41 <sup>d</sup> (37–47) <sup>a,d</sup>	45 <sup>d</sup> (44–45) <sup>a,d</sup>	43 (41–45) <sup>a</sup>	38 <sup>d</sup> (38–39) <sup>a,d</sup>	45 (42–51) <sup>a</sup>	49 (45–56) <sup>a</sup>
Q246C/L261C (29) <sup>b</sup> (sub 4) <sup>c</sup>	41 <sup>d</sup> (40–42) <sup>a,d</sup>	49 <sup>d</sup> (42–58) <sup>a,d</sup>	47 <sup>d</sup> (44–53) <sup>a,d</sup>	44 (38–61) <sup>a</sup>	47 <sup>d</sup> (44–52) <sup>a,d</sup>	39 (36–42) <sup>a</sup>	41 (38–44) <sup>a</sup>
Q137C/L261C (20) <sup>b</sup> (subs 1–4) <sup>c</sup>	47 <sup>d</sup> (44–52) <sup>a,d</sup>	32 <sup>d</sup> (31–33) <sup>a,d</sup>	39 <sup>d</sup> (37–41) <sup>a,d</sup>	36 (34–37) <sup>a</sup>	42 <sup>d</sup> (38–48) <sup>a,d</sup>	34 (34–34) <sup>a</sup>	34 (33–34) <sup>a</sup>
D288C/Q354C (29) <sup>b</sup> (subs 1–3) <sup>c</sup>	>55	>55 (58–) <sup>a</sup>	51 (51–52) <sup>a</sup>	44 (42–46) <sup>a</sup>	55 (52–58) <sup>a</sup>	43 (42–45) <sup>a</sup>	43 (41–45) <sup>a</sup>

<sup>a</sup> Values in parentheses represent the distance range appearing when the  $r_{01}$  values of the individual actin variants are used separately, one at a time. <sup>b</sup> Steady-state FRET distance (Å) between the  $\beta$ -carbons in the crystal structure. <sup>c</sup> Subdomains of actin that harbor the fluorophore (compare Figure 1). <sup>d</sup> Values collected from our earlier studies (16), repeated here for an easy overview and comparison between the bindings of actin to the chaperonins TRiC and GroEL.

the recognition of target molecules. Although GroEL is a chaperonin absent from eukaryotic cells, where actin is naturally present *in vivo*, studies have shown that GroEL recognizes and binds non-native actin (17, 18). GroEL is, however, not capable of guiding the actin molecule to its native state (17). It has been proposed that TRiC and GroEL recognize different folding intermediates of actin (18). Recalling that both GroEL and TRiC assist in the folding of target proteins by a binding-induced expansion mechanism, a very interesting question emerges. Is the nonproductive (in terms of assisting in folding) actin–GroEL interaction different from the actin–TRiC interaction, and if so, how does it differ and can a detailed description of the similarities and differences help to elucidate important details in the TRiC mechanism?

The actin–GroEL interaction was confirmed by >90% increased solubility of labeled actin and by increased fluorescein anisotropy (Figure 2), when actin is diluted into buffer containing GroEL. As shown in a previous study on the actin–TRiC interaction (16), the anisotropy ranges from

0.21 to 0.24 for the different variants when actin interacts with the large chaperonin complex. Here, similar measurements on the actin–GroEL complex were performed, giving rise to anisotropies of 0.18–0.29 for the single variants (Figure 2A–E), which should be interpreted as binding of actin (42 kDa) to the large chaperonin complex (800 kDa), giving rise to slow tumbling. Thus, we conclude that GroEL recognizes and binds denatured actin as it is diluted from 4 M GuHCl to folding conditions.

*Different Effects of Binding Actin to TRiC and GroEL: The Binding-Induced Expansion Seen in the Natural Actin–TRiC System Is a Vital Mechanism for the Folding of the Target Protein Actin.* As actin is diluted from denaturing conditions into a folding solution containing TRiC/ADP, it results in the binding and stretching of actin inside the TRiC cavity (16, 32). The stretching is in particular obvious when we look at the homo-FRET distance between the tips of subdomains 2 and 4 (Table 1, Figures 3B and 4), where positions 39 and 246 are situated (Figure 1). The present homo-FRET study clearly shows that the binding of non-

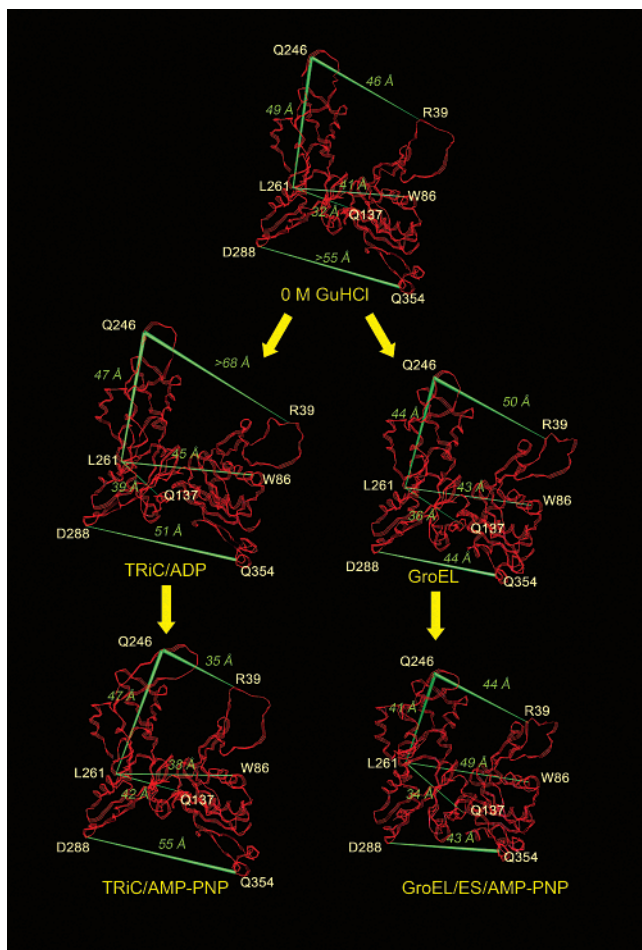


FIGURE 4: Flow scheme of the events in the actin molecule through the TRiC and GroEL chaperonin cycle. The structure alterations in the  $\beta$ -actin molecule were based on a merging of all data from the distance measurements. Green lines indicate the distances that were determined by homo-FRET measurements. The relative spatial positioning of the green distance lines represents the case in which the smallest possible change of the native structure is made to be compatible with all measured distances. The various actin structures are manually modified in a cartoonlike manner to fit with the indicated distances. Each distance is indicated by a number. The structure of native  $\beta$ -actin was modified in the various panels to be compatible with the merged data. As a reference, the structure of aggregation-prone actin intermediate in 0 M GuHCl is shown (top). As this intermediate binds to TRiC/ADP (middle left), it is stretched by binding-induced expansion. This major stretching is not seen in the binding to GroEL (middle right). Adding AMP-PNP to TRiC causes the chaperonin chamber to close. These conformational changes in the chaperonin affect the binding interactions to the actin molecule, leading to rearrangements in actin. Most pronounced is the compaction across the nucleotide-binding cleft. When AMP-PNP and GroES are added to GroEL, the chamber is closed, which leads to a slight compaction all over the actin molecule, except for in the middle (across the nucleotide-binding cleft), where in fact the distance is increased by 6 Å.

native actin to GroEL is far less dramatic compared to TRiC/ADP binding (Table 1 and Figure 3B). When we compare the 39–246 distance in actin bound to GroEL with the distances in the actin intermediate at 0 M GuHCl, the distance only increases by 4 Å in GroEL, compared to >22 Å in TRiC/ADP. This implies that, as non-native actin binds to GroEL, it is not stretched across the nucleotide-binding cleft in the same way as when actin binds to TRiC/ADP. Some other differences between the actin–TRiC/ADP and actin–

GroEL complexes are small; i.e., the 246–261 distance decreases by 2 Å upon binding of actin to TRiC/ADP, but decreases by 5 Å when actin is bound to GroEL. The 137–261 distance is increased by 7 Å when actin is bound to TRiC/ADP and by 4 Å when actin is bound to GroEL. The 86–261 distance, when actin is bound to GroEL (43 Å), only differs by 2 Å as compared to that of the TRiC/ADP-bound molecule (45 Å). Notably, the distance between positions 288 and 354 is remarkably long, >55 Å at 0 M GuHCl. As actin binds to TRiC/ADP, this distance decreases to 51 Å, while when actin binds to GroEL, the distance is even more compressed, to 44 Å. Figure 4 illustrates the expansion and compaction of the actin molecule through the chaperonin cycles of GroEL and TRiC, and the overall size differences are clearly seen in the “overlay” illustrations in Figure 5.

When the five calculated distances within the actin molecule in the initial binding to TRiC/ADP versus binding to GroEL are compared, an interesting overview on the effects of chaperonin action emerges. Three of the measured distances increase upon binding of actin to TRiC, and notably these distances also increase upon binding of actin to GroEL, but to a smaller degree. In addition, the locations of observed distance decreases are the same in the initial binding of actin to TRiC/ADP as in the actin–GroEL binding. In summary, the GroEL-bound actin molecule is overall more compact than TRiC/ADP-bound actin (Figures 4 and 5), which has much expanded outer parts compared to the GroEL-bound actin (Figure 5A). The 39–246 distance is >18 Å shorter in GroEL than in TRiC/ADP, and the 288–354 distance is 7 Å shorter. Less difference occurs between positions 86–261, 137–261, and 137–261, which are 2, 3, and 3 Å shorter in GroEL, respectively. The central core of actin thus seems to have similar compactness in both chaperonins. The differences in TRiC-bound and GroEL-bound actin could, at least partly, be a consequence of differences in the apical domains of TRiC and GroEL. In the apical domains of GroEL there are hydrophobic patches where the target proteins are proposed to interact (22–24, 33–35). The analogous sites in the TRiC subunit CCT $\gamma$  were shown to contain polar and charged amino acid residues (25). This observation has been a major argument for explaining the more selective recognition of target proteins by the eukaryotic chaperonin. We also speculate whether the size of the chaperonin contributes to the ability to selectively expand distinct regions of the target protein. GroEL is the smaller chaperonin complex, consisting of 14 subunits. The dimensions of the chaperonin are 150 Å (height)  $\times$  140 Å (width) (33, 36), and the diameter of the inner cavity is approximately 50 Å (33, 37). TRiC is a larger chaperonin complex, consisting of 16 subunits with total dimensions of 160 Å (height)  $\times$  150 Å (width) (32) and a cavity diameter of approximately 90 Å (32). Even if actin should bind to similar and corresponding positions in GroEL and TRiC/ADP, the initial stretching would not be as large in the GroEL cavity. Probably, the initial separation of distinct regions in actin is vital for the ability to reach the native structure, which will be further discussed below.

**Binding of ATP and GroES to the Actin–GroEL Complex Causes Smaller Rearrangements of Actin Than the Binding of ATP to the Actin–TRiC Complex.** GroEL is a group I chaperonin and works in conjunction with the co-chaperonin



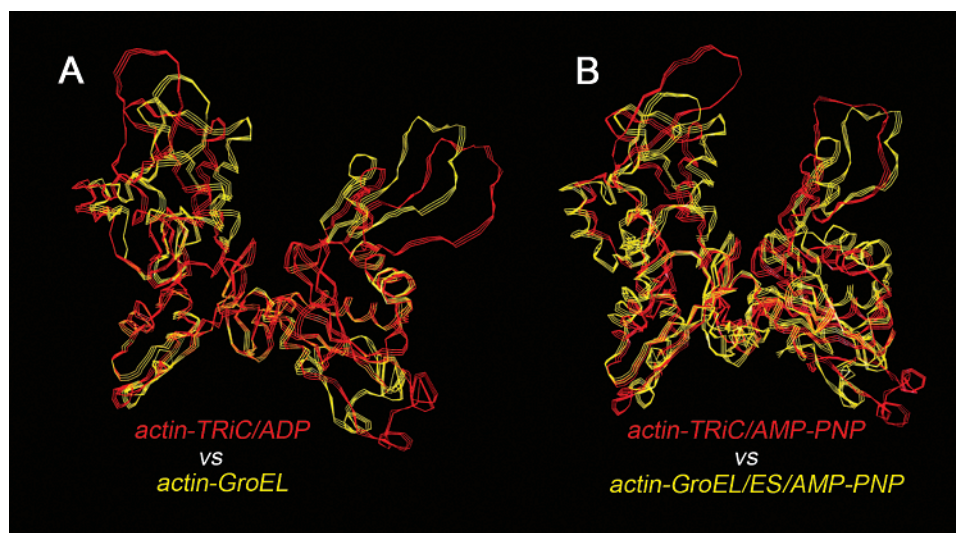


FIGURE 5: Structure overlay illustrating the differences in the actin structure when bound to TRiC/ADP vs GroEL (A) and TRiC/AMP-PNP vs GroEL/ES/AMP-PNP (B). (A) Comparison of actin bound to TRiC/ADP (red) and actin bound to GroEL (yellow). The illustration clearly shows that the actin molecule is more expanded in the TRiC/ADP chamber than in the GroEL chamber. This is particularly obvious across the nucleotide-binding cleft. (B) Comparison of actin in the TRiC/AMP-PNP chamber and the GroEL/ES/AMP-PNP chamber. Here, actin is expanded in the bottom of the molecule and vertically in TRiC/AMP-PNP compared to GroEL/ES/AMP-PNP. Importantly, the actin molecule is held together across the nucleotide-binding cleft to a higher degree in TRiC/AMP-PNP. The figure was constructed as described in the caption to Figure 4.

GroES, a ring-shaped protein complex with six identical 10 kDa subunits. During the chaperonin folding cycle, a target protein is first bound to one of the GroEL rings in its open (nucleotide-free) state. Then, as ATP binds to the equatorial domains of this ring, the intermediate domains rotate downward by  $20^\circ$ , which in turn leads to a large concerted change in the apical domains in the same ring, a  $\sim 25^\circ$  counterclockwise twist (38). These conformational changes have two consequences: (1) The hydrophobic surface (proposed to interact with the target protein during the initial binding) that is exposed in the nucleotide-free, target accepting state becomes partly buried into the intersubunit interface. (2) The cavity in which the target protein resides is enlarged (38). The change in the apical domains also seems to be important for GroES to recognize and bind to the chaperonin–target complex (38). GroES binds to the apical domains of GroEL, forming a lid to the chaperonin cavity. The binding of the co-chaperonin causes major movement in the apical domain, a  $60^\circ$  elevation and  $115^\circ$  clockwise twisting movement (37–39), giving rise to an even larger cavity. At this state of the GroEL/ES cycle, the target protein binding sites are completely hidden, and it has been proposed that the target protein is released into a chamber with hydrophilic walls.

To be able to monitor the effects of ATP and GroES binding by homo-FRET analysis, we used the nonhydrolyzable ATP analogue AMP-PNP to freeze the complex in a state before ATP hydrolysis. Thus, the measurements were performed on actin bound to GroEL, GroEL/AMP-PNP, and GroEL/ES/AMP-PNP, and the results are summarized in Table 1 and Figure 2A–E.

Note that TRiC does not work in conjunction with a co-chaperonin but has a built-in lid, which is closed in the ATP-bound state. Therefore, the actin–TRiC/AMP-PNP complex most closely corresponds to the actin–GroEL/ES/AMP-PNP complex, and comparisons will be made between them. Furthermore, a comparison of the actin–GroEL/AMP-PNP

and actin–GroEL/ES/AMP-PNP complexes show that they are very similar. The only notable difference is that the distance between positions 86 and 261 increases by 4 Å upon addition of GroES. The actin–TRiC/AMP-PNP complex will, partly for this reason, be compared with the GroES-containing complex.

Interestingly, as AMP-PNP and GroES are added to the actin–GroEL complex, the actin molecule becomes more compact because the homo-FRET measurements on the variants R39C/Q246C, Q246C/L261C, Q137C/L261C, and D288C/Q354C show a decrease in distance (Figure 4). (Notably, Lin and Rye have made similar observations for interactions of Rubisco with GroEL/ES (12).) However, the distance between positions 86 and 261 (which spans the bottom of the nucleotide-binding site in the actin molecule) is increased by 6 Å after addition of AMP-PNP and GroES to the actin–GroEL complex. In the corresponding TRiC complex, the corresponding distance is *decreased* by 7 Å when AMP-PNP is added. With this important difference in mind, we look closer at the R39C/Q246C variant, in which the probes are positioned to measure the distance between the large and small domains of actin at the entrance of the nucleotide-binding site. Here, the addition of AMP-PNP to the actin–TRiC complex leads to a collapse of actin, and the distance decreases from  $>68$  to a mere 35 Å, a distance very close to the native distance (Table 1). The corresponding change in the GroEL/ES/AMP-PNP complex is much smaller; the distance changes from 50 Å when actin is bound to GroEL to 44 Å in the GroEL/ES/AMP-PNP complex. In conclusion, subdomains 2 and 4 are held together in the TRiC/AMP-PNP chamber to a greater extent than in the analogous GroEL/ES/AMP-PNP chamber.

The large differences of the TRiC and GroEL action on the actin molecule across its nucleotide-binding site, shown in these homo-FRET measurements, support an early hypothesis that the TRiC chaperonin cycle is important for correct folding of the nucleotide-binding site. Our results

suggest that the stretching of actin in TRiC/ADP might unfold a misfolded substructure in a manner similar to that previously shown for GroEL and a target protein (7, 8). The stretching might also be necessary for accessibility and loading of ATP to the nucleotide-binding site in actin. We propose that the subsequent compaction of actin upon ATP binding to the chaperonin could be due to the binding of an ATP molecule to actin, which may stabilize a nativelike conformation of the nucleotide-binding cleft. This hypothesis is strengthened by the fact that when the nucleotide is removed from native actin, the native structure is lost and an aggregation-prone intermediate, I<sub>3</sub>, is formed (40). These results also suggest that loading of ATP to GroEL-bound actin is prohibited since the nucleotide-binding site is not accessible in any of the actin–GroEL complexes.

A second alternative is that the conformational changes in TRiC resulting from AMP-PNP binding actively push subdomains 2 and 4 toward each other and that they are forced to sit close in space due to mechanical action. These two mechanisms may also work in concert.

## CONCLUSIONS

It is apparent that the actin structure is rearranged by a binding-induced expansion mechanism in both TRiC and GroEL, but that binding to TRiC, in addition, causes a large separation of two subdomains, leading to a distinct expansion of the ATP-binding cleft in  $\beta$ -actin. A comparison of actin in the TRiC/AMP-PNP complex with actin in the GroEL/ES/AMP-PNP complex indicates that the GroEL system does not support formation of a functional structure at the nucleotide-binding cleft. Thus, the chaperonin cycles of TRiC and GroEL affect the actin molecule differently, and the binding-induced expansion of the ATP-binding cleft is vital for guiding actin to its native state.

## ACKNOWLEDGMENT

Ms. Kajsa Tibell is gratefully acknowledged for construction of Figures 4 and 5 based on merging of the data from the distance measurements.

## REFERENCES

- Sigler, P. B., Zhaohui, X., Rye, H. S., Burston, S. G., Fenton, W. A., and Horwich, A. L. (1998) Structure and function in GroEL-mediated protein folding, *Annu. Rev. Biochem.* 67, 581–608.
- Gutsche, I., Essen, L.-O., and Baumeister, W. (1999) Group II chaperonins: new TRiC(k)s and turns of a protein folding machine, *J. Mol. Biol.* 293, 295–312.
- Valpuesta, J. M., Martín-Benito, J., Gómez-Puertas, P., Carrascosa, J. L., and Willison, K. (2002) Structure and function of a protein folding machine: the eukaryotic cytosolic chaperonin CCT, *FEBS Lett.* 529, 11–16.
- Dunn, A. Y., Melville, M. W., and Frydman, J. (2001) Review: Cellular Substrates of the Eukaryotic Chaperonin TRiC/CCT, *J. Struct. Biol.* 135, 176–184.
- Klump, M., and Baumeister, W. (1998) The thermosome: archetype of group II chaperonins, *FEBS Lett.* 430, 73–77.
- Steinbacher, S., and Ditzel, L. (2001) Review: Nucleotide binding to the thermoplasma thermosome: Implications for the functional cycle of group II chaperonins, *J. Struct. Biol.* 135, 147–156.
- Persson, M., Hammarström, P., Lindgren, M., Jonsson, B. H., Svensson, M., and Carlsson, U. (1999) EPR mapping of interactions between spin-labeled variants of human carbonic anhydrase II and GroEL: evidence for increased flexibility of the hydrophobic core by the interaction, *Biochemistry* 38, 432–441.
- Hammarström, P., Persson, M., and Carlsson, U. (2001) Protein compactness measured by fluorescence resonance energy transfer. Human carbonic anhydrase II is considerably expanded by the interaction of GroEL, *J. Biol. Chem.* 276, 21765–21775.
- Hammarström, P., Persson, M., Owenius, R., Lindgren, M., and Carlsson, U. (2000) Protein substrate binding induces conformational changes in the chaperonin GroEL. A suggested mechanism for unfoldase activity, *J. Biol. Chem.* 275, 22832–22838.
- Persson, M., Aronsson, G., Bergenhem, N., Freskgard, P. O., Jonsson, B. H., Surin, B. P., Spangfort, M. D., and Carlsson, U. (1995) GroEL/ES-mediated refolding of human carbonic anhydrase II: role of N-terminal helices as recognition motifs for GroEL, *Biochim. Biophys. Acta* 1247, 195–200.
- Persson, M., Carlsson, U., and Bergenhem, N. (1997) GroEL provides a folding pathway with lower apparent activation energy compared to spontaneous refolding of human carbonic anhydrase, *FEBS Lett.* 411, 43–47.
- Lin, Z., and Rye, H. (2004) Expansion and compression of a protein folding intermediate by GroEL, *Mol. Cell* 16, 23–34.
- Rommelaere, H., Van Troys, M., Gao, Y., Melki, R., Cowan, N. J., Vandekerckhove, J., and Ampe, C. (1993) Eukaryotic cytosolic chaperonin contains t-complex polypeptide 1 and seven related subunits, *Proc. Natl. Acad. Sci. U.S.A.* 90, 11975–11979.
- Chen, X., Sullivan, D. S., and Huffaker, T. C. (1994) Two yeast genes with similarity to TCP-1 are required for microtubule and actin function in vivo, *Proc. Natl. Acad. Sci. U.S.A.* 91, 9111–9115.
- Spiess, C., Meyer, A. S., Reissmann, S., and Frydman, J. (2004) Mechanism of the eukaryotic chaperonin: protein folding in the chamber of secrets, *Trends Cell Biol.* 14, 598–604.
- Villebeck, L., Persson, M., Luan, S.-L., Hammarström, P., Lindgren, M., and Jonsson, B. H. (2007) Conformational rearrangements of tail-less complex polypeptide 1 (TCP-1) ring complex (TRiC)-bound actin, *Biochemistry* 46, 5083–5093.
- Tian, G., Vainberg, I. E., Tap, W. D., Lewis, S. A., and Cowan, N. J. (1995) Specificity in chaperonin-mediated protein folding, *Nature* 375, 250–253.
- Melki, R., and Cowan, N. J. (1994) Facilitated folding of actins and tubulins occurs via a nucleotide-dependent interaction between cytoplasmic chaperonin and distinctive folding intermediates, *Mol. Cell. Biol.* 14, 2895–2904.
- Persson, M., Carlsson, U., and Bergenhem, N. C. (1996) GroEL reversibly binds to, and causes rapid inactivation of, human carbonic anhydrase II at high temperatures, *Biochim. Biophys. Acta* 1298, 191–198.
- Riddles, P. W., Blakely, R. L., and Zerner, B. (1983) Reassessment of Ellman's reagent, *Methods Enzymol.* 91, 49–60.
- Hamman, B. D., Oleinikov, A. V., Jokhadze, G. G., Traut, R. R., and Jameson, D. M. (1996) Dimer/monomer equilibrium and domain separations of Escherichia coli ribosomal protein L7/L12, *Biochemistry* 35, 16680–16686.
- Fenton, W. A., Kashi, Y., Furtak, K., and Horwich, A. L. (1994) Residues in chaperonin GroEL required for polypeptide binding and release, *Nature* 371, 614–619.
- Buckle, A. M., Zahn, R., and Fersht, A. R. (1997) A structural model for GroEL-polypeptide recognition, *Proc. Natl. Acad. Sci. U.S.A.* 94, 3571–3575.
- Chen, L., and Sigler, P. B. (1999) The crystal structure of a GroEL/peptide complex: Plasticity as a basis for substrate diversity, *Cell* 99, 757–768.
- Pappenberger, G., Wilsheer, J. A., Roe, S. M., Counsell, D. J., Willison, K. R., and Pearl, L. H. (2002) Crystal structure of the CCT? Apical domain: Implications for substrate binding to the eukaryotic cytosolic chaperonin, *J. Mol. Biol.* 318, 1367–1379.
- Hynes, G. M., and Willison, K. R. (2000) Individual subunits of the eukaryotic cytosolic chaperonin mediate interactions with binding sites located on subdomains of beta-actin, *J. Biol. Chem.* 275, 18985–18994.
- Llorca, O., McCormack, E., Hynes, G., Grantham, J., Cordell, J., Carrascosa, J. L., Willison, K. R., Fernández, J. J., and Valpuesta, J. M. (1999) Eukaryotic type II chaperonin CCT interacts with actin through specific subunits, *Nature* 402, 693–696.
- McCormack, E. A., Llorca, O., Carrascosa, J. L., Valpuesta, J.-M., and Willison, K. (2001) Point mutations in a hinge linking the small and large domains of  $\beta$ -actin result in trapped folding intermediates bound to cytosolic chaperonin CCT, *J. Struct. Biol.* 135, 198–204.
- Feldman, D. E., Spiess, C., Howard, D. E., and Frydman, J. (2003) Tumorigenic mutations in VHL disrupt folding in vivo by interfering with chaperonin binding, *Mol. Cell* 12, 1213–1224.



30. Kubota, S., Kubota, H., and Nagata, K. (2006) Cytosolic chaperonin protects folding intermediates of Gbeta from aggregation by recognizing hydrophobic beta-strands, *Proc. Natl. Acad. Sci. U.S.A.* 103, 8360–8365.
31. Spiess, C., Miller, E. J., McClellan, A. J., and Frydman, J. (2006) Identification of the TRiC/CCT substrate binding sites uncovers the function of subunit diversity in eukaryotic chaperonins, *Mol. Cell* 24, 25–37.
32. Llorca, O., Martín-Benito, J., Grantham, J., Ritco-Vonsovici, M., Willison, K. R., Carrascosa, J. L., and Valpuesta, J. M. (2001) The 'sequential allosteric ring' mechanism in the eukaryotic chaperonin-assisted folding of actin and tubulin, *EMBO J.* 20, 4065–4075.
33. Braig, K., Otwinowski, Z., Hegde, R., Boisvert, D. C., Joachimlak, A., Horwich, A. L., and Sigler, P. B. (1994) The crystal structure of the bacterial chaperonin GroEL at 2.8 angstroms, *Nature* 371, 578–586.
34. Hlodan, R., Tempst, P., and Hartl, F. U. (1995) Binding of defined regions of a polypeptide to GroEL and its implications for chaperonin-mediated protein folding, *Nat. Struct. Biol.* 2, 587–595.
35. Kobayashi, N., Freund, S. M., Chatellier, J., Zahn, R., and Fersht, A. R. (1999) NMR analysis of the binding of a rhodanese peptide to a minichaperone in solution, *J. Mol. Biol.* 292, 181–190.
36. Igarashi, Y., Kimura, K., Ichimura, K., Matsuzaki, S., Ikura, T., Kuwajima, K., and Kihara, H. (1995) Solution X-ray scattering study on the chaperonin GroEL from Escherichia coli, *Biophys. Chem.* 53, 259–266.
37. Xu, Z., Horwich, A. L., and Sigler, P. B. (1997) The crystal structure of the asymmetric GroEL-GroES-(ADP)<sub>7</sub> chaperonin complex, *Nature* 388, 741–750.
38. Ranson, N. A., Farr, G. W., Roseman, A. M., Gowen, B., Fenton, W. A., Horwich, A. L., and Saibil, H. R. (2001) ATP-bound states of GroEL captured by cryo-electron microscopy, *Cell* 107, 869–879.
39. Chaudhry, C., Farr, G. W., Todd, M. J., Rye, H. S., Brunger, A. T., Adams, P. D., Horwich, A. L., and Sigler, P. B. (2003) Role of the gamma-phosphate of ATP in triggering protein folding by GroEL-GroES: function, structure and energetics, *EMBO J.* 22, 4877–4887.
40. Altschuler, G. M., Klug, D. R., and Willison, K. (2005) Unfolding energetics of G-a-actin: A discrete intermediate can be re-folded to the native state by CCT, *J. Mol. Biol.* 353, 385–396.
41. van den Ent, F., Amos, L. A., and Löwe, J. (2001) Prokaryotic origin of the actin cytoskeleton, *Nature* 413, 39–44.
42. Turoverov, K. T., Verkhusha, V. V., Shavlovsky, M. M., Biktashev, A. G., Povarova, O. I., and Kuznetsova, I. M. (2002) Kinetics of actin unfolding induced by guanidine hydrochloride, *Biochemistry* 41, 1014–1019.

BI700658N